International Research Journal of Engineering and Technology (IRJET) e-ISSN: 2395-0056
Volume: 10 Issue: 07 | July 2023 www.irjet.net p-ISSN: 2395-0072

# DC MICROGRID USING PHOTOVOLTAIC IMPROVED INCREMENTAL CONDUCTANCE ALGORITHM FOR TRACKING THE MPP IN A STAND-ALONE MINIMIZING ENERGY STORAGE UTILIZATION

**Mr. Mandli Vamshidhar Reddy[1], Dr.Sivaganesan Sivanantham[2]**

*[1]PG Scholar in electrical power systems department of electrical and electronics engineering at Holy Mary Institute of Technology and Science, Bogaram, Medchal Dist, Hyderabad, India.*
*[2]Professor of electrical and electronics engineering at Holy Mary Institute of Technology and Science, Bogaram, Medchal Dist, Hyderabad, India.*

---

**Abstract -** This paper proposes a versatile and ideal control procedure for a sunlight based photovoltaic (PV) framework. The control procedure guarantees that the sun based PV board is generally opposite to daylight and all the while worked at its most extreme power point (MPP) for constantly reaping greatest power. A mixture control technique for a PV and battery energy capacity framework (BESS) in an independent dc MG is proposed in this paper. Rather than the traditional control methodologies that manage the dc-interface voltage just with the BESS, the proposed control procedure takes advantage of both the PV framework and the BESS to direct the dc-connect voltage. The proposed control methodology is the control blend between the solar powered trackers (ST) and (MPPT) that can enormously work on the produced power from sun based PV frameworks. As to ST framework, the paper presents two drive approaches including shut circle drives. The paper likewise proposes Incremental conductance (InC) calculation for improving the speed of the MPP following of a sun oriented PV board under different climatic circumstances as well as ensuring that the working point generally moves towards the MPP utilizing this proposed calculation. The viability of the proposed control methodology on delaying the lifetime of a lithium-particle battery and a lead-corrosive battery is examined through a reenactment contextual investigation with one-day burden and irradiance bend profiles.

***Key Words***: Battery energy storage system (BESS), battery state-of-charge (SoC), dc microgrid (dc MG), improved incremental conductance power point tracking (InCPPT) algorithm photovoltaic (PV).

## 1. INTRODUCTION

Energy is absolutely essential for our life and demand has greatly increased worldwide in recent years. The research efforts in moving towards renewable energy can solve these issues. Compared to conventional fossil fuel energy sources, renewable energy sources have the following major advantages: they are sustainable, never going to run out, free and non-polluting. Renewable energy is the energy generated from renewable natural resources such as solar irradiation, wind, tides, wave, etc. Amongst them, solar energy is becoming more popular in a variety of applications relating to heat, light and electricity. It is particularly attractive because of its abundance, renewability, cleanliness and its environmentally-friendly nature. One of the important technologies of solar energy is photovoltaic (PV) technology which converts irradiation directly to electricity by the PV effect. However, it can be realized that the solar PV panels have a few disadvantages such as low conversion efficiency (9% to 17%) and effects of various weather conditions [1]. In order to overcome these issues, the materials used in solar panel manufacturing as well as collection approaches need to be improved. Obviously, it is particularly difficult to make considerable improvements in the materials used in the solar PV panels.

Renewable energy resources are rapidly replacing conventional fuels to generate electricity in order to achieve energy sustainability, and reduce the carbon footprint [1]. Solar energy is one of the most abundantly available renewable resources and hence, photovoltaic (PV) power generation share is steadily increasing. DC microgrid (dcMG) power systems are drawing great attention due to the steady growth in dc load demand and renewable dc sources. The majority of modern consumer electronics such as energy-efficient lighting systems and energy-saving electronics are operated with dc supply. Furthermore, PV modules and batteries are intrinsically dc components. Therefore, by using a dcMG to transfer power from dc sources to dc loads would eliminate the necessity of having dc-to-ac conversion stages on the generation side and ac-to-dc conversion stages on the load side. Also, synchronization and reactive power flow issues are null in dcMGs [2], [3]. Such dc systems are used in a broad range of applications including ships, automobiles, telecommunication stations, etc. However, issues associated with dynamically changing weather conditions and dc-link voltage transients may lead to instability in the microgrid and hence, dcMGs require a robust control scheme. The majority of existing PV controllers aim to extract the maximum power from the PV arrays using maximum power point tracking (MPPT)

algorithms [4], [5], and the battery energy storage system (BESS) deals with the power difference between the load and the PV generation. Nowadays, with falling PV energy cost, supersizing the PV capacity just for the purpose of having more PV energy during the afternoon hours is a common practice and makes perfect economic sense in many cases [6], [7], [8], [9]. As the PV capacity increases, its effect on grid parameters will increase as well. Therefore, the PV system should play a bigger role by participating in grid stabilization. When the PV capacity increases, MPPT operation may cause dc-link over-voltage and the BESS overcharging issues. Hence, the MPPT method alone is insufficient to control the PV generation and additional features are needed to help maintain the dc-link voltage [6]. The excessive PV penetration issue is solved with MPPT droop dual-mode control strategy with the BESS [10], [11], [12], [13]. However, the controller for the PV generation

Therefore, increasing of the irradiation intensity received from the sun is an attainable solution for improving the performance of the solar PV panels. One of the major approaches for maximizing power extraction in solar PV systems is a sun tracking system. The sun tracking systems were introduced in [2]-[3] using a microprocessor, and in [4] using a programmable logic controller respectively. The closed-loop control schemes for automatic sun tracking of double-axis, horizon single-axis, and fixed systems were presented and compared in [5]. Furthermore, the idea of designing and optimizing a solar tracking mechanism was also proposed in [6]. Additionally, it can also be realized that the V-I characteristic of the solar cell is non-linear and varies with irradiation and temperature [1]. Generally, there is a unique point on the V-I or V-P curve which is called the Maximum Power Point (MPP). This means that the solar PV panel will operate with a maximum efficiency and produce a maximum output power. The MPP is not known on the V-I or V-P curve, and it can be located by search algorithms such as the Perturbation and Observation (P&O) algorithms [7]-[12], the Incremental Conductance (InC) algorithm [13]-[14], the Constant Voltage (CV) algorithm [15]-[16], the Artificial Neural Network (ANN) algorithm [17]-[18], the Fuzzy Logic (FL) algorithm [19]-[20], and the Particle Swarm Optimization (PSO) algorithm [21]-[24]. These existing algorithms have several advantages and disadvantages concerned with simplicity, convergence speed, extra-hardware and cost. This paper proposes an improved InC algorithm for tracking a MPP on the V-I characteristic of the solar PV panel. Based on the ST and MPPT, the solar PV panel is always guaranteed to operate in an adaptive and optimal situation for all conditions. The remainder of this paper is organized as follows.

The mathematical model of solar PV panels is described in Section II. A proposal for adaptive and optimal control strategy of a solar PV panel based on the control combination of the solar tracker (ST) and MPP tracker (MPPT) with the improved InC algorithm is presented in Section III. The simulation and experimental results then follow to confirm the validity of the proposal in Sections IV and V. Finally, the advantages of the proposal are summarized through a comparison with other solar PV panels. Development and Comparison of an Improved Incremental Conductance Algorithm for Tracking the MPP of a Solar PV Panel.

## 2. CIRCUIT CONFIGURATION

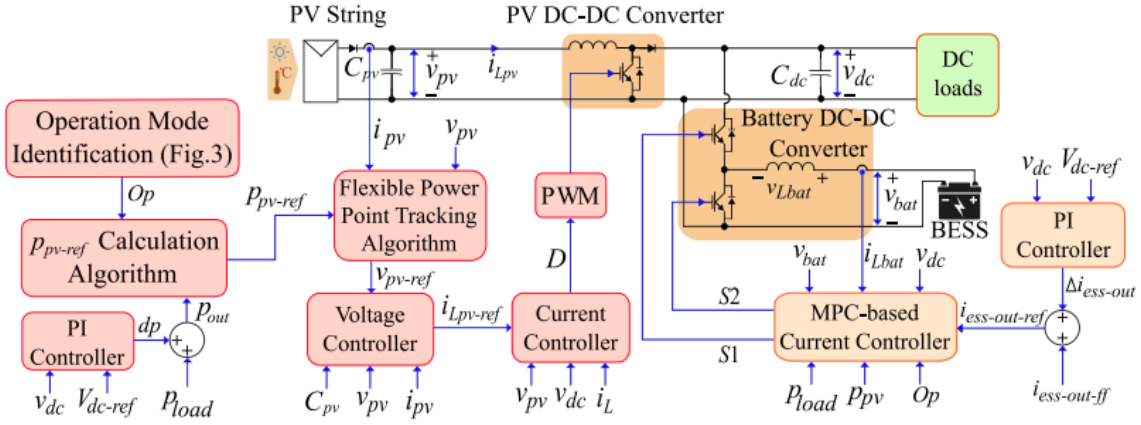


Fig. 1. Circuit configuration and proposed control strategy of the standalone hybrid DCMG.

In [10] generates disturbances on the dc-link voltage during operation mode transitions and the transition criteria itself complicates the control algorithm. The PV controller in [11] only focuses on the dc-link voltage regulation, and the algorithm in [12] only focuses on the MPPT operation mode. Therefore, an additional outer-loop controller is required to extract the maximum power from the PV in [11], and to regulate the dc-link voltage in [12]. An MPPT and droop integrated control method is introduced in [13] to eliminate the system disturbances by avoiding the control

reconfiguration during operation mode transitions. The droop controller regulator is the key element in the control that provides a duty ratio for the dc-dc converter by calculating the required change of the power with the droop coefficient. However, the PV controllers in [10], [11], [12], [13] operate with the constant voltage-step to adjust the PV generation, resulting a slow dynamic response under rapid environmental changes. Hence, the battery is the primary dc-link voltage controller and operates continuously (charge/discharge) to effectively regulate the dc voltage fluctuations, which are mainly imposed by the load demand transients and the intermittent irradiance changes. Such aggressive utilization severely degrades the battery lifetime [14], [15].

The proposed control techniques for dcMGs in [16], [17], [18] did not consider reducing the battery utilization and the excessive use of battery power to regulate the dc-link voltage is a drawback that drastically shortens the battery lifetime. Furthermore, the forecast-based control proposed in [19] limits the state-of-charge (SoC) to an estimated SoC reference, which is predicted based on the load demand patterns, to prolong the battery lifetime. However, the control involves with the online communication platform for the forecasting data and it is only effective in the grid-connected system since it limits the battery charging capacity. In the stand-alone dcMG system, the battery is the only available backup source when the PV generation is absent and hence, the SoC needs to be kept high. To solve the above mentioned drawbacks, this paper proposes a control strategy for a stand-alone dcMG system with PV and BESS. In the proposed hybrid control strategy, the PV system is the primary dc-link voltage regulator and the BESS acts as a secondary dc voltage control asset that can remain in standby mode as long as the PV is able to maintain the dc voltage within a desired range and the battery does not need to charge. This control hierarchy, thus prolongs the battery lifetime by minimizing the utilization of the BESS.

The proposed control strategy keeps the SoC of the battery within a desired range, provided enough power is available from the PV. With the help of the PV system, the average daily number of charge/discharge cycles of the battery is reduced. The proposed controller operates based on the premise of keeping the BESS off while it is full and the instantaneous PV power is sufficient to meet the load demand. Hence, on average, the operating temperature of the BESS is reduced, which helps extending its lifetime. The BESS converter is forced to operate only if: (i) the SoC of the battery drops below a pre-defined limit (which translates that the battery needs to restore energy), (ii) transient dc-link voltage deviates beyond the allowed limits, and (iii) the load demand exceeds the available power from the PV. When the BESS is operative, the PV generates its maximum power. Otherwise, the PV power is regulated to match the load demand by a fast flexible power point tracking (FPPT) algorithm with adaptive voltage-step calculation [6], [7], [8]. The transient performance of the proposed algorithm is evaluated with experimental results and its effectiveness to prolong the battery lifetime is tested under a randomly selected one-day load and irradiance profiles. The structure of this paper is as follows: the details of the proposed control strategy is introduced in Section II, experimental demonstration is done in Section III. A case study to evaluate the effect of proposed control strategy on battery lifetime is provided in Section IV, and the conclusions of the paper are stated in Section V.

## 3. PROPOSED CONTROL STRATEGY

The circuit configuration of an islanded dcMG powered by a PV power plant and the BESS is shown in Fig. 1. The proposed hybrid control strategy, the PV converter controller, and the BESS converter controller are explained in detail in the following subsections.

### *A. Proposed Hybrid Control Strategy*

The main objective of the proposed control strategy is to treat the battery as the secondary source in the islanded dcMG, which is used only when the maximum PV power is insufficient to fulfill the load demand. The battery also helps to regulate the dc-link voltage *vdc* if it deviates beyond a predefined voltage limits during transients. These limits define a

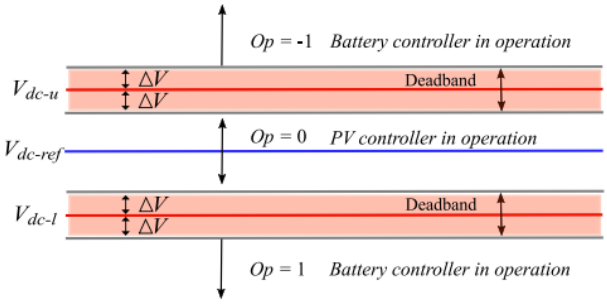


Fig. 2. Proposed operation control limits.

Voltage band in which only the PV controller regulates the dclink voltage whereas, if *vdc* is not within this voltage band, the BESS converter will operate to help regulating the dc voltage. Here, *Vdc-u* and *Vdc-l* are the upper and lower limits of the dc-link voltage, respectively, which define the voltage band as shown in Fig. 2. There is also a deadband around each of these control limits denoted by *V*. These deadbands are set to prevent the battery from turning on and off recursively around the boundary limits. The PV maximum power *ppv-max* is estimated using the approach in [9]. *Op* represents the battery operation mode (*Op* = -1 shows charge mode, *Op* = 0 shows standby mode and *Op*=1 shows discharge mode) and *pload* is the load power. Subsequently, the battery SoC level is etimated using (1).

$$SoC(k) = SoC(k - 1) - (kkT - s1)Ts(ibat/Cbat)\, dt, \quad (1)$$

where *k* is the sample number, *Ts* is the time-step, *ibat* is the battery current, and *Cbat* is the battery capacity. If the battery current is negative (current is flowing towards the battery), the SoC will increase and vice versa, the SoC will decrease if *ibat* is positive (battery is discharging). The rate of SoC change is directly proportional to *ibat*.

As shown in Fig. 3, if *pload* is larger than the maximum available power *ppv-max*, *(pload > ppv-max)*, the BESS will operate and discharge the stored energy (*Op* = 1, discharge mode) as the load demand is higher than the maximum power supply from the PV. Otherwise, *Op* will be updated accordingly based on the dc-link voltage *vdc* fluctuation. For instance, if *vdc* is greater than *Vdc-u +V*, the battery regulates the dclink voltage by absorbing the power from the dc bus (*Op*=-1, charge mode). Similarly, if *vdc* is smaller than *Vdc-l - V*, shown in Fig. 3, the battery discharges as *vdc* deviation is out of the allowed band and thereby, *vdc* is regulated by the BESS to the innermost boundaries, *Vdc-u - V* and *Vdc-l + V*.

This function is added to the controller to ensure the stability of the dcMG under sudden large step changes of the load, during which the PV converter may not provide the required fast transient response. Once the battery is able to regulate the dc-link voltage *vdc* into the innermost boundaries, the battery SoC is compared with its reference value *SoCth*. If the SoC is lower than *SoCth*, *Op* is updated to -1 and the battery is put into operation (charge mode) to be charged by the PV excess power generation (*ppv-max - pload*). Once the battery SoC reaches to

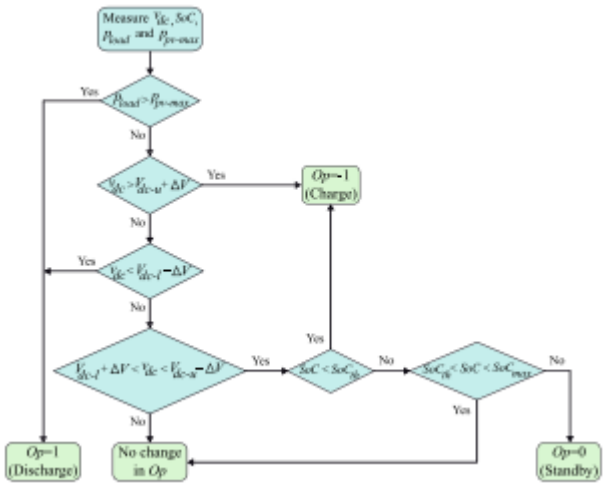


Fig. 3. Proposed hybrid operation mode identification strategy.

*SoCmax*, the battery controller is switched off (*Op*=0, standby mode) and only the PV converter controller is responsible for converging *vdc* to its reference value *Vdc-ref*. Such threshold range (where the battery does not need to charge), as shown in Fig. 3, is implemented to reduce the micro-cycle operations when the load transients occur frequently. If *vdc* is within the deadband zones, *Op* value will not be updated.

When determining *SoCth* value, there are numerous factors that need to be considered (i.e., types of battery and their chemical characteristics, charge/discharge rate, working temperature, SoC level and the load profile). Higher *SoCth* value will increase the number of micro-cycles while the lower value risks having lower stored energy. With the proposed control methodology, the BESS utilization and the number of partial charge/discharge cycles is substantially reduced. As a result, the battery lifetime is prolonged. According to the above discussions and the flowchart in Fig. 3, the following conditions need to be satisfied in order to keep the battery in the standby mode: (i) the battery SoC is higher than *SoCth* (which translates that the battery does not need to charge), (ii) PV system has sufficient power for the load demand (*ppv-max > pload*), and (iii) *vdc* fluctuation is within the pre-defined voltage limits (PV is able to regulate *vdc* to its reference value *vdc-ref* ). The PV power reference *ppv-ref* is given by: *ppv-ref* = *pp*load *pv-max* + *dp* , , *Op Op* = = 00 (2) The PV controller collects the *Op*, *ppv-max* and *pload* information to determine *ppv-ref* . If *Op* is not 0, the battery is in operation and thus, *ppv-ref* is set to *ppv-max*. Hence, the PV operates at its maximum power point in order to either reduce the load share of the BESS as much as possible (when *pload > ppv-max*), or to restore the battery SoC to *SoCmax* (when the battery needs to restore energy). If *Op* is 0, it translates that the battery is not in operation. Thus, the PV will completely take control of *vdc* regulation by adjusting

## 4. SIMULATION RESULTS

The performance of the proposed control strategy is verified experimentally under intermittent irradiance changes and different loading conditions with a hardware setup shown in Fig. 4. The parameters of the experimental setup are provided in Table. I. The results in this section are based on the assumption of having a constant PV cell temperature of 25 ◦C. As shown in Fig. 5, there are two possible operating points for the PV power reference *ppv-ref*: Point A on the left-side of the

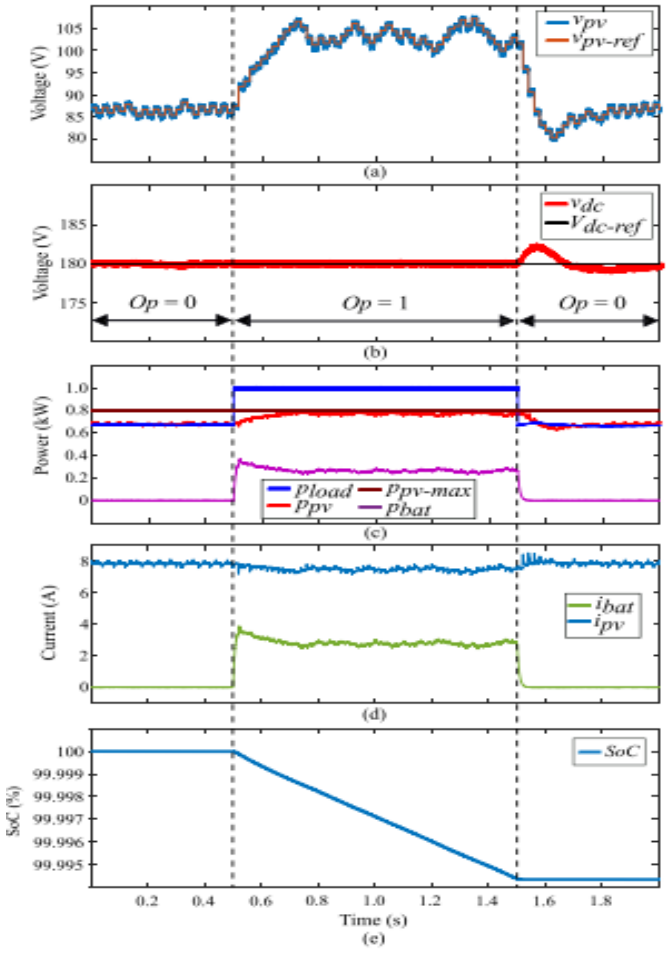


Fig. 6. *Case I*: Experimental verification of the transient response of the proposed control strategy under different loading conditions. (a) PV voltage, (b) dc-link voltage, (c) PV power, PV maximum power, load power and battery power, (d) PV and battery currents, and (e) SoC. maximum power point (MPP) and point B on the right-side of the MPP [7], [8]. Operating at the right-side of the MPP provides a faster dynamic response than operating at the left side as a small PV voltage change results in a large power deviation. However, the disadvantage is that the PV output power will have a higher oscillation even at the steady-state condition. If the PV operates at the left-side of the MPP, the PV output power benefits from lower power oscillation at the cost of slower dynamic performance as compared to the rightside of MPP operation. In the experimentation, the controller limits the PV operation to the left-side of the MPP to attain the low power oscillation while the dynamic is enhanced by utilizing variable voltage-step.

*Case I*: In this case study, the performance of the proposed control strategy under different loading conditions is examined and results are shown in Fig. 6. The SoC threshold limit *SoCth*

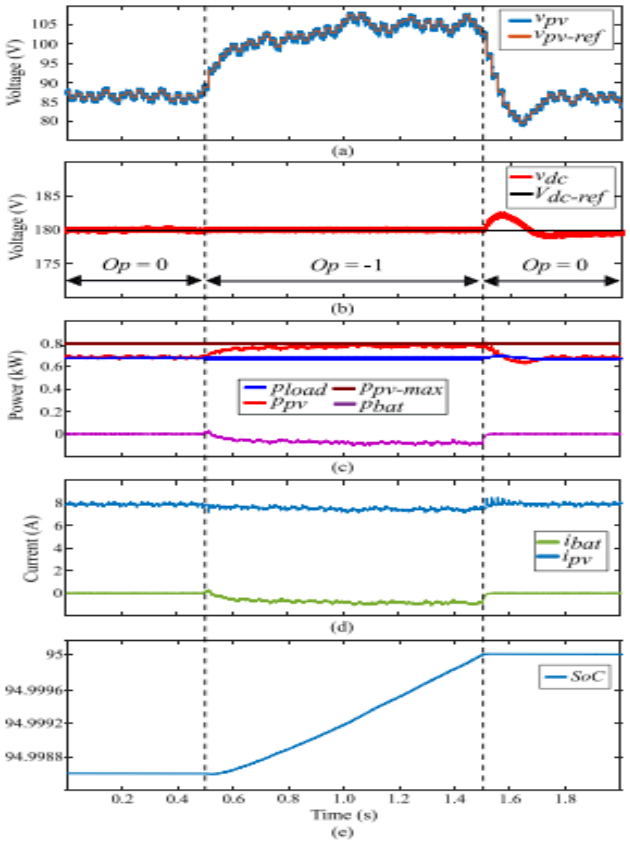


Fig. 7. *Case II*: Experimental results of the battery SoC preservation in a desired operation range. (a) PV voltage, (b) dc-link voltage, (c) PV power, PV maximum power, load power and battery power, (d) PV and battery currents, and (e) SoC. is emulated to be smaller than the battery SoC in this case (*SoC>SoCth*). Initially, the PV is supplying power according to the load demand of 650 W and the battery is also not operating as the load demand is below *ppv-max (*800 W*)* and the SoC is larger than *SoCth*. At *t* = 0.5 s, *pload* suddenly increases from 650 W to 1000 W as illustrated in Fig. 6(b). Since *pload* is larger than *ppv-max*, the operation status *Op* is updated to 1, shown in Fig. 6(b). Hence, the PV increases its output power to the maximum available power and the battery converter is also in operation to supply the remaining load demand from the battery. At the instant of load change *(t* = 0.5 s*)*, the battery current supply increases as shown in Fig. 6(d). At the same time, the PV supply increases to its maximum power at the steady-state. Then, the load power *pload* reduces back to 650 W at *t* = 1.5 s. During this condition, since the PV has sufficient capacity to supply the demand and the battery SoC is still larger than its reference value (*SoC >SoCth*), the operation status *Op* is updated to 0. Hence, the battery converter is disconnected from the system in order to reduce its utilization. From then, only the PV system regulates the dclink voltage *vdc* to its reference value *vdc-ref* , as shown in Fig. 6(b). This case study demonstrates the capability of the proposed control strategy in supplying the load demand with reduced battery utilization.

*Case II*: This case study shows the use of the proposed hybrid control strategy to maintain the SoC within its predefined limits, as shown in Fig. 7. The initial SoC threshold limit *SoCth* is emulated to be below the SoC of the battery (*SoC*>*SoCth*) and the load demand is fixed at 650 W. Initially, the PV is generating the load demand and the battery system is not in action. An increase in *SoCth*, which is higher than the battery SoC (*SoC* < *SoCth*), is emulated at *t* = 0.5 s.

Subsequently, the operation mode *Op* is updated to -1 based on the proposed strategy in Fig. 3, as depicted in Fig. 7(b). Thus, the output of the PV is increased to the maximum possible value and any surplus generation from the PV system is supplied to the battery in order to increase the SoC, as demonstrated in Figs. 7(c) and (d). At *t* = 1.5 s, the battery SoC reaches its maximum limit *SoCmax* (95 % in this case). As a result, *Op* is updated to 0 and *ppv-ref* is set to the load demand plus the power deviation from the dc-link voltage regulation, described in (2). The BESS is also disconnected from the system and its current becomes zero, as shown in Fig. 7(d). In this case, it can be observed that the proposed hybrid control strategy successfully executes the function of keeping the SoC within the desired operating range.

*Case III*: The performance of the proposed control strategy is investigated under the fast linear irradiance variations as depicted in Fig. 8. The load demand is constant at 650 W and the irradiance is initially at 1 kW/m2. The battery SoC is larger than the emulated *SoCth* (*SoC* > *SoCth*). Thus, the PV power is equivalent to the load demand and the BESS does not operate. At *t* = 14.5 s, the irradiance linearly drops to 0.5 kW/m2 and the PV supply is consequently reduced as shown in Fig. 8(b). Since the load demand is larger than the maximum supply from the PV, *Op* is updated to 1 to fulfill the load demand as shown in Fig. 8(c). Subsequently, the battery converter seizes to operate when the irradiance increases back to 1 kW/m2 at *t* = 35.5 s because the PV has sufficient generation to cater for the load demand and the battery SoC is still larger than its threshold limit *SoCth*. This demonstrates the dynamic performance and robustness of the proposed control strategy to rapid irradiance changes.

## 5. ANALYSIS OF BATTERY LIFE IMPROVEMENT

In order to evaluate the effectiveness of the proposed control strategy, load and irradiance profiles for one day, as shown in Fig. 9, are utilized in this case study. Firstly, battery lifetime estimation models are provided and afterwards, the estimated battery lifetime by using the conventional control strategy [11], [16], [21] and proposed control strategy are compared. The working temperature of the battery is one of the factors that leads to rapid degradation of the battery lifetime [14],

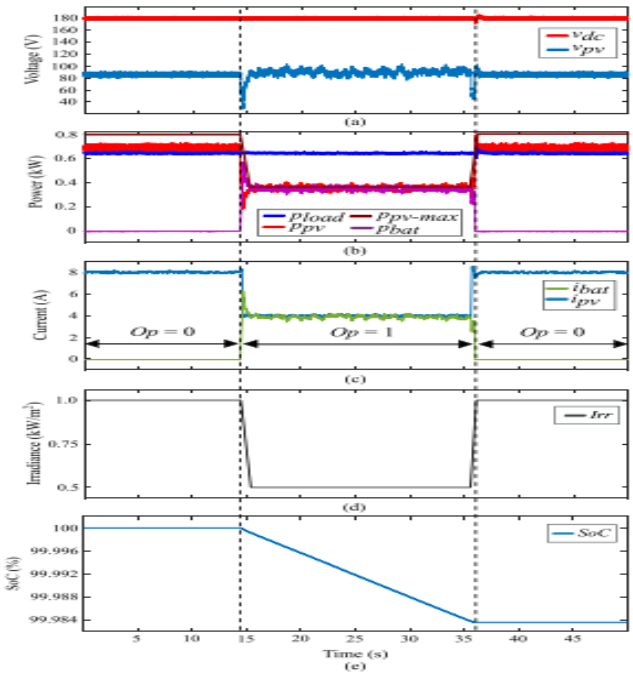


Fig. 8. *Case III*: Experimental investigation of the proposed control strategy under intermittent irradiance changes. (a) PV voltage, and dc-link voltage, (b) PV power, PV maximum power, load power and battery power, (c) PV and battery currents, (d) irradiance and (e) SoC. [15].

As the current flows in and out of the battery, power dissipates as heat in the internal resistance of the battery. The internal battery temperature *Tin* is estimated by the heat transfer thermal resistance in this case study. The parameters of the selected Lithium-ion (Li-ion) battery (3.3 V, 70 Ah) are provided in [22]. The battery capacity is designed in such a way that the battery is effectively utilized (SoC variation between 100 % max. and 20 % min.). Accordingly, there are four parallel strings of 16 battery banks connected in series. Each battery bank has 70 m internal series resistance [23].

This resistance value is used to calculate the internal power losses of the battery. An electrical equivalent circuit thermal model is implemented to analyze the battery cell temperature as shown in Fig. 10. *Tamb* is the ambient temperature and it is assumed to be 25 ◦C. In the following, the lifetime study is repeated for another common battery type, i.e., lead-acid (LA) battery. The battery lifetime is estimated based on the same load demand, PV generation, and battery utilization manners of the proposed and the conventional controls, as presented in Figs. 11 and 12. The rating of each LA cell is 2 V, 4 Ah and there are ten parallel strings of 30 battery banks connected in series. The overall heat transfer coefficient is 5.7 WK-1m-2 for the thermal resistance from the cell to the surroundings. The thermodynamic properties of this battery are provided in [26]. Subsequently, the temperature/current dependence

characteristic (9), which is experimentally analyzed in [26], is used to estimate the LA

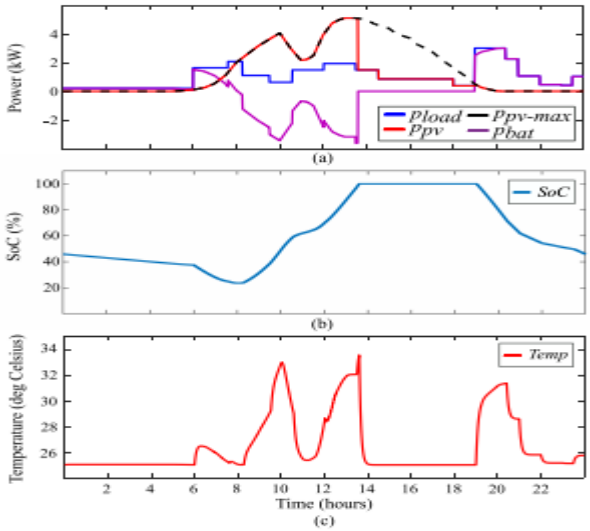


Fig. 11. Simulation results of the proposed control strategy under a one day case study. (a) Load power, PV power, PV maximum power and battery power, (b) SoC, and (c) temperature. Battery cell temperature. $T = 36.2I + 25$ (9) among the different LA battery degradation parameters, temperature is known to be the most impactful parameter. Hence, the remaining lifetime of the LA battery *LLA* is where *Ln* is the nominal life of the LA battery, *(ti - ti-1)* is the time difference, *Ti* is the average temperature during the time period *ti*, *Tx* is the temperature at time period *tx*, and $\alpha$=10 is the change in temperature coefficient. Accordingly, the LA battery can last for 1112 days with the proposed control strategy and 778 days with the conventional control strategy before reaching the EoL. It is also noted that the lifetime of the LA battery is relatively shorter than the Li-ion battery [28]. Thus, this case study exhibits that the proposed control strategy prolongs the Li-ion battery aging, based on different battery degrading parameters, by 29.93 % as compared to the conventional control strategy (from 1964 days in the conventional control to 2552 days in the proposed control). Similarly, the gained lifetime of the LA battery with the proposed control strategy is around 42.93 % (from 778 days in the conventional control to 1112 days in the proposed control). Hence, the proposed control strategy demonstrates the significance of

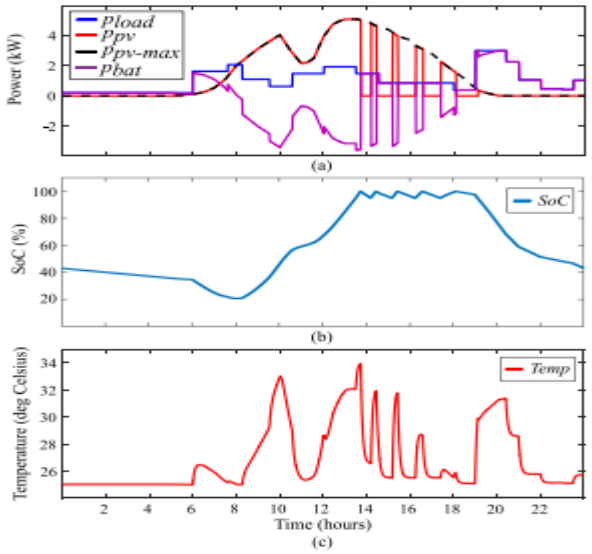


Fig. 12. Simulation results of the conventional control strategy under an one day case study. (a) Load power, PV power, PV maximum power and battery power, (b) SoC, and (c) temperature. Having FPPT capability for the PV systems in stand-alone dcMGs.

## CONCLUSION

In this paper, it is obvious that the adaptive and optimal control strategy plays an important role in the development of solar PV systems. This strategy is based on the combination between the ST and MPPT in order to ensure that the solar PV panel is capable of harnessing the maximum solar energy following the sun's trajectory from dawn until dusk and is always operated at the MPPs with the improved InC algorithm. The proposed InC algorithm improves the conventional InC algorithm with an approximation which reduces the computational burden as well as the application of the CV algorithm to limit the search space and increase the convergence speed of the InC algorithm. This improvement overcomes the existing drawbacks of the InC algorithm. The paper also proposes an improved incremental conductance (InC) algorithm for enhancing the speed of the MPP tracking of a solar PV panel under various atmospheric conditions as well as guaranteeing that the operating point always moves towards the MPP using this proposed algorithm. The effectiveness of the proposed control strategy on prolonging the lifetime of a lithium-ion battery and a lead-acid battery is investigated via a simulation case study with one-day load and irradiance curve profiles

## REFERENCES

[1] R. Faranda and S. Leva, "Energy comparison of MPPT techniques for PV systems," *WSES Trans. Power Syst.*, vol. 3, no. 6, pp. 446–455, 2008.

[2] X. Jun-Ming, J. Ling-Yun, Z. Hai-Ming, and Z. Rui, "Design of track control system in PV," in *Proc. IEEE Int. Conf. Softw. Eng. Service Sci.*, 2010, pp. 547–550.

[3] Z. Bao-Jian, G. Guo-Hong, and Z. Yan-Li, "Designment of automatic tracking system of solar energy system," in *Proc. 2nd Int. Conf. Ind. Mechatronics Autom.*, 2010, pp. 689–691.

[4] W. Luo, "A solar panels automatic tracking system based on OMRON PLC," in *Proc. 7th Asian Control Conf.*, 2009, pp. 1611–1614.

[5] W. Chun-Sheng, W. Yi-Bo, L. Si-Yang, P. Yan-Chang, and X. Hong-Hua, "Study on automatic sun-tracking technology in PV generation," in *Proc. 3rd Int. Conf. Elect. Utility Deregulation Restruct. Power Technol.*, 2008, pp. 2586–2591.

[6] C. Alexandru and C. Pozna, "Different tracking strategies for optimizing the energetic efficiency of a photovoltaic system," in *Proc. Int. Conf. Autom., Quality Testing, Robot.*, 2008, pp. 434–439.

[7] R. Sridhar, S. Jeevananthan, N. T. Selvan, and P. V. Sujith Chowdary, "Performance improvement of a photovoltaic array using MPPT P&O technique," in *Proc. Int. Conf. Control Comput. Technol.*, 2010, pp. 191– 195.

[8] N. M. Razali and N. A. Rahim, "DSP-based maximum peak power tracker using P&O algorithm," in *Proc. IEEE 1st Conf. Clean Energy Technol.*, 2011, pp. 34–39.

[9] L. Chun-Xia and L. Li-qun, "An improved perturbation and observation MPPT method of photovoltaic generate system," in *Proc. 4th IEEE Conf. Ind. Electron. Appl.*, 2009, pp. 2966–2970.

[10] Y. Jung, J. So, G. Yu, and J. Choi, "Improved perturbation and observation method (IP&O) of MPPT control for photovoltaic power systems," in *Proc. 31st IEEE Photov. Spec. Conf.*, 2005, pp. 1788–1791.

[11] G. C. Konstantopoulos and A. T. Alexandridis, "Non-linear voltage regulator design for DC/DC boost converters used in photovoltaic applications: Analysis and experimental results," *IET Renew. Power Gen.*, vol. 7, pp. 296–308, May 2013.

[12] A. Tofighi and M. Kalantar, "Power management of PV/battery hybrid power source via passivity-based control," *Renew. Energy*, vol. 36, pp. 2440–2450, Sep. 2011.

[13] H. Cai, J. Xiang, W. Wei, and M. Z. Q. Chen, "V-dp/dv droop control for PV sources in DC microgrids," *IEEE Trans. Power Electron.*, vol. 33, no. 9, pp. 7708–7720, Sep. 2018.

[14] P. Ruetschi, "Aging mechanisms and service life of lead–acid batteries," *Power Sources*, vol. 127, pp. 33–44, Mar. 2004.

[15] B. Shabani and M. Biju, "Theoretical modelling methods for thermal management of batteries," *Energies*, vol. 8, pp. 10153–10177, Sep. 2015.

[16] H. Mahmood, D. Michaelson, and J. Jiang, "Decentralized power management of a PV/battery hybrid unit in a droop-controlled islanded microgrid," *IEEE Trans. Power Electron.*, vol. 30, no. 12, pp. 7215–7229, Dec. 2015.

[17] Y. Shan, J. Hu, K. W. Chan, Q. Fu, and J. M. Guerrero, "Model predictive control of bidirectional DC–DC converters and AC/DC interlinking converters—A new control method for PV-wind-battery microgrids," *IEEE Trans. Sustain. Energy*, vol. 10, no. 4, pp. 1823–1833, Oct. 2019.

[18] T. Dragicevic, J. M. Guerrero, J. C. Vasquez, and D. Škrlec, "Supervisory control of an adaptive-droop regulated DC microgrid with battery management capability," *IEEE Trans. Power Electron.*, vol. 29, no. 2, pp. 695–706, Feb. 2014.

[19] G. Angenendt, S. Zurmühlen, H. Axelsen, and D. U. Sauer, "Comparison of different operation strategies for PV battery home storage systems including forecast-based operation strategies," *Appl. Energy*, vol. 229, pp. 884–899, Nov. 2018.

[20] A. Narang *et al.*, "An algorithm for fast flexible power point tracking in photovoltaic power plants," in *Proc. 45th Annu. Conf. IEEE Ind. Electron. Soc. (IECON)*, vol. 1. Lisbon, Portugal, Oct. 2019, pp. 4387–4392.

[21] Y. Yang, Y. Qin, S.-C. Tan, and S. Y. R. Hui, "Efficient improvement of photovoltaic-battery systems in standalone DC microgrids using a local hierarchical control for the battery system," *IEEE Trans. Power Electron.*, vol. 34, no. 11, pp. 10796–10807, Nov. 2019.

[22] Y. Xiao, "Model-based virtual thermal sensors for lithium-ion battery in EV applications," *IEEE Trans. Ind. Electron.*, vol. 62, no. 5, pp. 3112–3122, May 2015.

[23] *Li-Ion Battery Datasheet*, EEMB, Hongkong, 2021. [Online]. Available: https://www.ineltro.ch/media/downloads/SAAItem/45/45958/36e3e7f3-2049-4adb-a2a7-79c654d92915.pdf

[24] B. Xu, A. Oudalov, A. Ulbig, G. Andersson, and D. S. Kirschen, "Modeling of lithium-ion battery degradation for cell life assessment," *IEEE Trans. Smart Grid*, vol. 9, no. 2, pp. 1131–1140, Mar. 2018.

[25] M. Musallam and C. M. Johnson, "An efficient implementation of the rainflow counting algorithm for life consumption estimation," *IEEE Trans. Rel.*, vol. 61, no. 4, pp. 978–986, Dec. 2012.

**Author details:**

**Mr. Mandli Vamshidhar Reddy** received a B.Tech in electrical and electronics engineering from Bharat Institute of Engineering and Technology (BIET), Ibrahimpatnam, Ranga Reddy Dist. And studying M.tech in electrical power systems at Holy Mary Institute of Technology and Science, Bogaram, Medchal Dist, Hyderabad, India in the dept. electrical and electronics engineering.

**Dr.Sivaganesan Sivanantham** received the B.E. in Electrical and Electronics Engineering from University of Madras, TN in2003and M.Tech.in Power Electronics & Drives from SASTRA University, TN in 2006and the Ph.D. degree in Electrical Engineering from Vels University, Tamil nadu in 2017. He is currently an HoD & Professor of Dept. of Electrical & Electronics Engineering at Holy Mary Institute of Technology and Science, Hyderabad. His research interests include photovoltaic systems, renewable energy systems, power electronics, and control of power electronics interfaces.